Physical Layer Simulation Results for IEEE 802.11p using Vehicular non-Stationary Channel Model

Laura Bernadó[1], Nicolai Czink[1], Thomas Zemen[1], Pavle Belanović[2]

[1]Forschungszentrum Telekommunikation Wien (FTW), Vienna, Austria
[2]Universidad Politécnica de Madrid, Madrid, Spain
Contact: bernado@ftw.at

***Abstract*—Traffic safety can be improved by using a vehicular dedicated communication protocol. The standard IEEE 802.11p is being developed for this purpose. The physical layer properties of this draft are based on the already widely used IEEE 802.11a standard. Nevertheless, the propagation conditions in vehicular communications are different to the ones considered for 802.11a, which is focusing on nomadic indoor usage, and well studied until now. In this paper we present the simulation results obtained from an implemented physical layer model for this standard. The used channel model describes the very peculiar characteristics of the vehicular radio channel, specially the non-stationarity. Several channel estimators are tested based on the pilot structure defined in the standard focusing on low complexity implementations. The results show that diffuse components, present in vehicular channels on highways, have a very significant impact on the system performance. Furthermore, in situations of poor line-of-sight contribution, an acceptable frame error rate is not achievable even at high signal-to-noise ratio values. Therefore, more complex channel estimation and equalization techniques based on the current standard pilot pattern have to be developed that are able to cope with the properties of the vehicular radio channel.**

I. Introduction

In the recent years, vehicular communications have raised interest due to the fact that they can help reduce traffic accidents and traffic jams. The IEEE is currently working on the new 802.11p standard, dedicated to vehicular communications. The draft specifies special implementation of the medium access control (MAC) and the physical (PHY) layer. In order to implement receiver algorithms with good performance, simulations have to be performed using realistic channel models. Up to now, several groups have been investigating the results of the 802.11p standard from the MAC-layer perspective [1], [2]. However, the PHY layer analysis has not been thoroughly investigated, yet. A bit-error-rate analysis has been presented in [3], where the authors consider two basic vehicle-to-vehicle communications in highway and urban scenarios. Only one kind of channel estimation technique was tested, and that only in non-vehicular stationary models.

In this paper we present a performance evaluation of different basic channel estimation and equalization techniques in terms of frame error rate (FER). Several channel models representing the vehicular radio channel properties have been developed recently [4]. We use a realistic non-stationary vehicular channel model parametrized directly from measurements at 5 GHz. Since we are interested in the communication of safety related messages, we focus on the infrastructure-to-vehicle (I2V) communication between vehicles and the road operators' infrastructure.

This research was supported by the project REALSAFE, as well as the project COCOMINT funded by Vienna Science and Technology Fund (WWTF), and the EC under the FP7 Network of Excellence projects NEWCOM++. The Telecommunications Research Center Vienna (FTW) is supported by the Austrian Government and the City of Vienna within the competence center program COMET.

II. System Description

In this section we give a brief overview of the 802.11p standard, describe the used estimation techniques, and the non-stationary vehicular channel model.

A. System Overview

We implemented a PHY-layer simulator transmission chain 802.11p standard compliant. In the standard there are 8 different coding and modulation schemes defined. Each one achieves different data rates. Only three of them are mandatory to be implemented. In order to transmit the randomly generated data in the simulation we choose the coding-modulation scheme achieving 6 Mbps. This uses QPSK modulation and a convolutional code with constraint length 7 at a coding rate of $1/2$. This is one of the most robust transmission schemes, and the results will be worse for the other, less protected schemes. Zero forcing is used as equalization method. Since vehicular channels are strong time-varying, channel estimation has a severe impact in the system performance.

B. Estimation Techniques

The results presented in this paper show the system performance of the 802.11p standard employing regular estimation and equalization techniques. The 802.11p pilot pattern considers two kind of pilots: block, and comb pilots [5]. The pilot allocation is shown in Fig. 1. All 52 subcarriers of the first two OFDM symbols are dedicated to pilots. Afterwards, only 4 subcarriers contain pilots throughout the whole frame duration. These so-called comb pilot subcarriers have indices $6, 20, 33$, and 47. Based on them, we define three different type of channel estimators: block, comb, and block-comb. Within these categories, the investigated techniques are:

- *Block-type channel estimators:* An estimate of the channel is calculated from the block pilots. The estimated channel coefficients are used for the whole frame. They

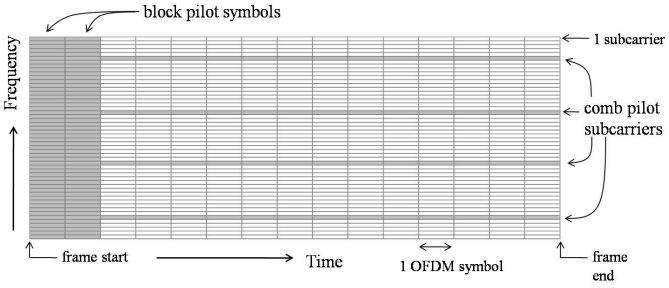

Fig. 1. Pilot allocation in IEEE 802.11p.

do not take time variation into account. We investigate the effect of least-squares (LS) channel estimation

$$\hat{\mathbf{h}}_{B-LS} = \mathbf{X}_p^{-1}\mathbf{y}_{p1,p2}, \tag{1}$$

and minimum mean square error (MMSE) estimation

$$\hat{\mathbf{h}}_{B-MMSE} = \mathbf{R}_{HH}\mathbf{X}_p^H \left(\mathbf{X}_p\mathbf{R}_{HH}\mathbf{X}_p^H + \sigma^2\mathbf{I}\right)^{-1}\mathbf{y}_{p1,p2}, \tag{2}$$

referred as to block LS (B-LS) and block MMSE (B-MMSE) estimators [6], [7], [8]. In (1), $\mathbf{y}_{p1,p2}$ has a form of a vector with the pilots of the two first received blocks stacked, and $\mathbf{X}_p^T = [\mathbf{X}_{p1}\mathbf{X}_{p2}]$, where $\mathbf{X}_{p1,p2}$ are diagonal matrices containing the pilot symbols. In (2) $\mathbf{R}_{HH}$ is the channel frequency correlation function, and σ^2 is the noise variance. We use the estimated channel coefficients for every instance of the frame.

- *Comb-type channel estimators:* Only the four pilot subcarriers are used to obtain a LS estimate of the channel at the comb positions. The channel coefficients for the rest of the subcarriers are calculated using interpolation techniques. We consider linear, and spline interpolation. The resulting channel estimators under this category are comb LS with linear interpolation (CLS-linear), and comb LS with first order spline interpolation (CLS-spline) [8], [9], [10].
- *Block-comb-type channel estimators:* An initial channel estimate is calculated based on the block pilots using the LS technique. Subsequently, a linear MMSE filtering in the time domain is applied. We propose two channel estimators, block-comb MMSE 1 (BC-MMSE$_1$) that assumes the time correlation function $\mathbf{R}_{hh}$ based on the Clarke's model [11], and block-comb MMSE 2 (BC-MMSE$_2$) that estimates the time correlation function $\hat{\mathbf{R}}_{\hat{h}\hat{h}}$ from the comb pilots. Both are described by

$$\hat{\mathbf{H}}_{BC-MMSE_1} = \mathbf{R}_{hh}\mathbf{X}_p^H \left(\mathbf{X}_p\mathbf{R}_{hh}\mathbf{X}_p^H + \sigma^2\mathbf{I}\right)^{-1}\mathbf{Y}, \tag{3}$$

where $\mathbf{Y}$ is a matrix containing the received symbols at the pilot positions. For BC-MMSE$_2$, the channel time correlation function is estimated as

$$\hat{\mathbf{R}}_{\hat{h}\hat{h}} = \frac{1}{P}\sum_{p=1}^{P}\hat{\mathbf{h}}_p\hat{\mathbf{h}}_p^H, \tag{4}$$

where P is the number of pilot subcarriers and $\hat{\mathbf{h}}_p$ is the estimated channel frequency response at the comb pilot positions for all time instances using LS.

These techniques have been used in other communication systems with good results [6], [7], [8], [9], [10]. Our objective is to check if they are also suitable for vehicular communications or whether more sophisticated techniques need to be implemented. From an implementation point of view it is important to take the complexity of the different channel estimators into account. Figure 2 shows the number of floating-point operations (flops) needed per frame of length 200 bytes for the different channel estimators.

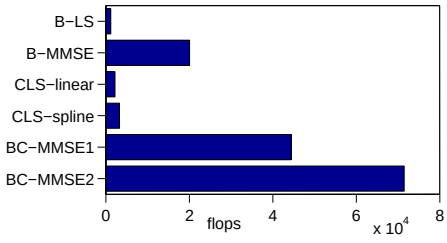

Fig. 2. Number of floating point operations needed for different channel estimators.

C. Non-Stationary Channel Model

The channel model adopted by the 802.11p standard is a tap delay line model. However, this model does not accurately represent the most important features of the vehicular radio channel [4].

Dedicated vehicular radio channel measurements at 5 GHz have shown that the main contributions in the channel impulse response are: line-of-sight (LOS), deterministic scattering, and diffuse scattering. The LOS component has a strong power as long as there is a direct connection between transmitter (Tx) and receiver (Rx). It drops to lower power values due to shadowing when there is an obstructing object. The diffuse scattering contribution has a significant impact on the channel power. A very important characteristic of vehicular channels is that different delays present correlated fading due to reflections coming from the same object along time. The statistical properties of the channel change over time and therefore the channel is non-stationary. All these characteristics are not taken into account in the model proposed for 802.11p. For this reason, we use a geometry-based stochastic channel model [4] directly parameterized from vehicular measurements at 5.2 GHz [12] which models all of these effects, and thus leads to trustworthy simulation results.

We generate a typical highway vehicular scenario. It consists of a road-side unit acting as Tx, a vehicle acting as Rx, discrete scattering objects (mobile and static, MD and SD), and diffuse scattering (D) at both sides of the road. The mobile discrete scatterers symbolize other cars moving on the road, while the static discrete scatterers represent traffic signs. The diffuse scattering wall models foliage and other objects present along the road. The position of the scatterers is randomly determined. The speed of the mobile discrete scatterers is

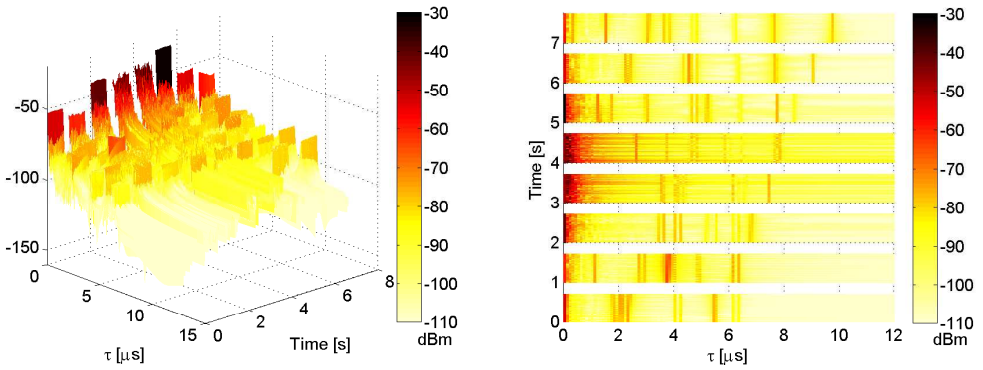

(a) 3D representation (b) 2D representation

Fig. 3. Channel impulse response.

stochastically assigned from a distribution with a mean of 90 km/h and a standard deviation of 2 km/h. Tx and Rx are deterministically placed. The velocity of the Rx is set to 100 km/h. Since we want to simulate a I2V scenario, the Tx does not move and is located in the middle of the road. The time-varying channel transfer function is calculated as

$$\begin{aligned} H(f,t) =& \gamma^{(\mathrm{LOS})}(t)\exp[-j2\pi f\tau^{(\mathrm{LOS})}(t)]+ \\ & \sum_{k=1}^{N_{\mathrm{SD}}}\gamma_k^{(\mathrm{SD})}(t)\exp[-j2\pi f\tau_k^{(\mathrm{SD})}(t)]+ \\ & \sum_{k=1}^{N_{\mathrm{MD}}}\gamma_k^{(\mathrm{MD})}(t)\exp[-j2\pi f\tau_k^{(\mathrm{MD})}(t)]+ \\ & \sum_{k=1}^{N_{\mathrm{D}}}\gamma_k^{(\mathrm{D})}(t)\exp[-j2\pi f\tau_k^{(\mathrm{D})}(t)], \end{aligned} \tag{5}$$

where $\gamma_k^{(\cdot)}$ denote the complex-valued attenuation coefficient of the different paths, which include the effects of path loss, antenna patterns, and large-scale fading. $\tau_k^{(\cdot)}$ denote the delays of the paths, and $N_{(\cdot)}$ denote the numbers of SD, MD and D scatterers, respectively.

The Tx sends 100 frames, each having 200 bytes, every second during 7 seconds. In 7 seconds the Rx covers a distance of 200 m. Between transmissions Tx and Rx remain silent. This allows us to calculate FER over time. A 3D and 2D representation of the envelope of the generated impulse responses are depicted in Fig. 3 (a) and (b) respectively. The

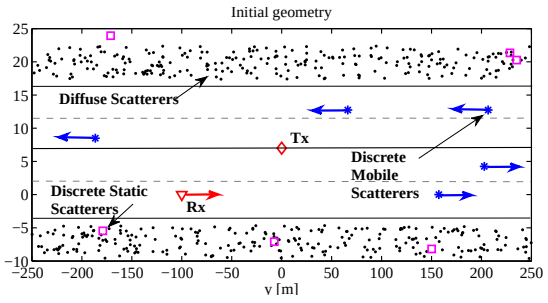

Fig. 4. Scatterers distribution over 500 m.

duration of the transmission of 100 frames of 200 bytes is 29.6 ms. In order to see the channel impulse response, the transmission time in Fig. 3 is scaled a factor of 30.

The Rx approaches the Tx from 0 to 3 s. During this time, the impulse response shows a very well defined LOS component and other contributions appearing at later delays. A similar behaviour is observed from 5 to 7 s. Noteworthy is to mention that at time 1 s the LOS component has a very low power due to shadowing. The contributions from the other delays are stronger and therefore resulting in a larger delay spread. On the other hand, at 5 s the LOS is very strong, and thus the effective delay spread is shorter. From 3 to 4 s the Rx drives by the Tx. At this point, the influence of the diffuse components becomes important and can be noticed on the distribution of the channel power in the delay. After the LOS, we observe a diffuse tail which increases the delay spread of the channel.

III. Results

We simulate the transmission of 100 frames every second in the scenario shown in Fig. 4, over which we calculate the FER. We consider that the Tx transmits with constant power. The maximum signal-to-noise ratio (SNR) achieved is 40 dB. Since the channel model includes the path loss, the SNR varies in time. Figure 5 depicts the FER over time for the different estimation and equalization techniques presented in Section II. At the bottom of Fig. 5 we plot the time evolution of the SNR at the Rx. At time 5 s, the SNR is 40 dB and maximal.

The channel estimator BC-MMSE$_1$ results in a FER of 1 during almost the whole simulated time. This is because this estimator assumes a given channel correlation function, which is based on a non-LOS model, while the current I2V communication scenario is mainly LOS. Assuming the wrong statistical properties of the channel leads to a high error rate.

As already commented in Fig. 3, at 1 s the channel has a very weak LOS component due to shadowing and also a large delay spread. None of the tested channel estimators can cope with these bad channel conditions. Regardless of the used technique, no frame is decoded correctly. On the other hand, at 5 s the LOS component is very strong and the estimation can

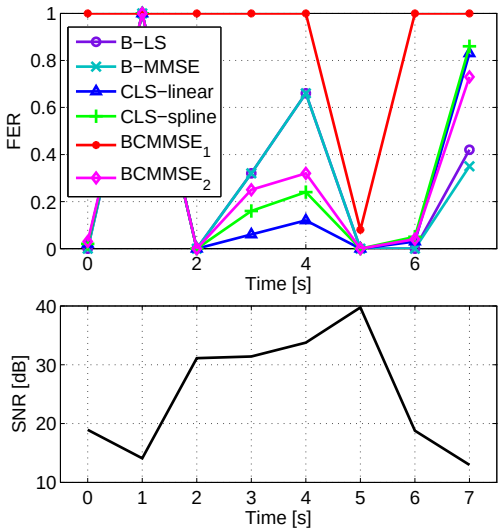

Fig. 5. Comparison of different channel estimators and equalizers. FER over time for a maximal SNR of 40 dB.

be performed satisfactorily. Therefore a FER of 0 in almost all tested cases is achieved.

If we focus now on seconds 3 and 4, we observe a significant performance difference between the estimators. During this time interval the effect of the diffuse component becomes relevant. Even though we have a higher SNR at 3 and 4 s, the FERs achieved are lower in average than the ones achieved at 6 s, where the SNR is much lower. This points out the influence of the diffuse components in the channel estimation performance.

The estimation technique achieving the worst FER are the block-based channel estimators. Since the SNR at these instances is still high, above 30 dB, there is no performance difference between B-LS and B-MMSE.

The BC-MMSE$_2$ estimator follows the block type estimators achieving a FER below 0.3. In this case, the estimation of the channel time-correlation function provides a good estimate of the time-variability of the channel. This improves the performance of a simple block pilot based channel estimator. The two estimators performing best in this area are the comb-pilot-based estimators. By using the four pilot-dedicated subcarriers, CLS-linear and CLS-spline get a very good estimate of the phase evolution during the frame.

Figure 6 shows the true and the estimated channel transfer function for subcarrier 21 for one channel realization. In Fig. 6 (a) and (b), the channel phase and magnitude are plotted. These channel estimators that take into account time evolution are able to estimate a changing phase and magnitude. This is the case for CLS-linear, CLS-spline, and BC-MMSE$_2$. As commented before, BC-MMSE$_1$ also accounts for time variability, but not correctly, therefore we see a wrong time evolution in phase and magnitude. For the block-based channel estimators no time variation is considered. In Fig. 6 (c), the real and imaginary part of the true and estimated channel transfer function are plotted. There we see that the closest

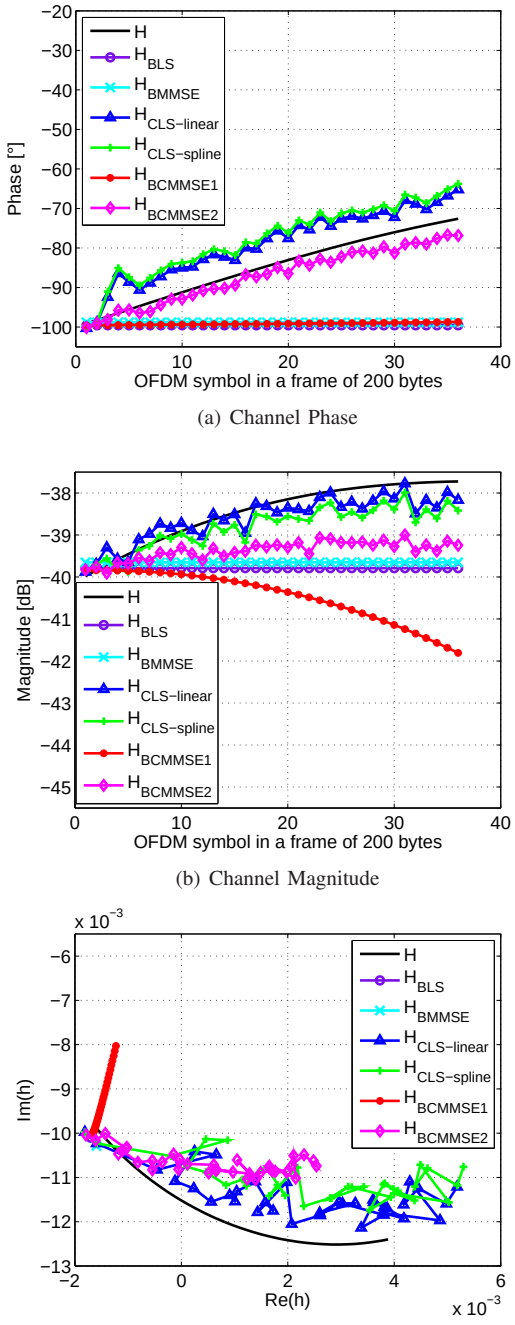

(a) Channel Phase

(b) Channel Magnitude

(c) Channel

Fig. 6. Estimated and true channel for subcarrier 21 at time 4 s for a maximal SNR of 40 dB (SNR$_{4s}$ = 33.5 dB.)

approximation to the true channel is given by the comb-type channel estimators. Although the tendency in the time evolution of the phase is well estimated in these cases, in subfigure 6 (a) we see that there is an offset with respect to the true phase. Since we are using a QPSK modulation, as long as the phase offset is within ± 45 degrees; the Rx decides for the correct symbol. Figure 7 presents the average phase offset per subcarrier over the 100 transmitted frames at 4 s. With a modulation where the symbols are closer, the FER will increase. We observe in this figure as well that there is

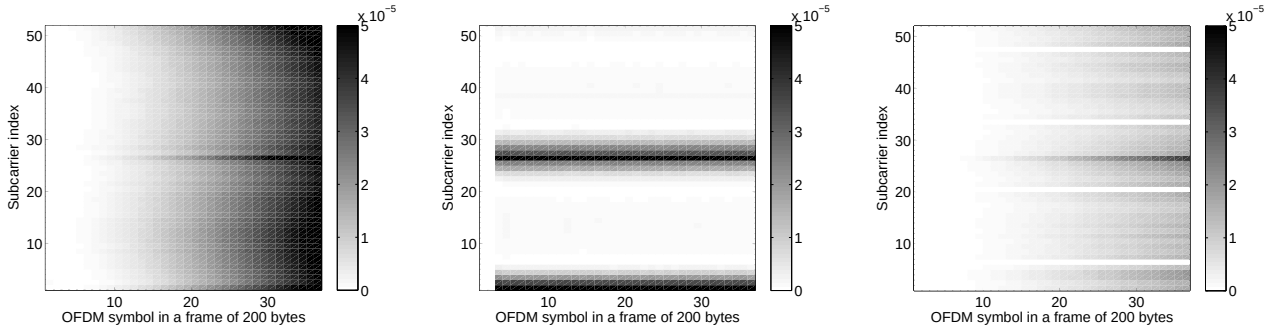

(a) B-MMSE (b) CLS-linear (c) BC-MMSE$_2$

Fig. 8. Time-frequency MSE at 4 s for a maximal SNR of 40 dB (SNR$_{4s}$ = 33.5 dB.)

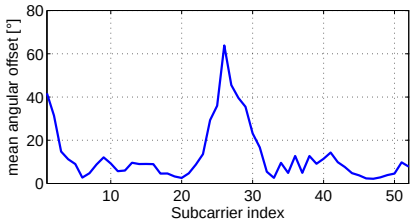

Fig. 7. Average phase offset per subcarrier for CLS-linear channel estimator at 4 s.

a range of subcarriers where the interpolation does not work properly. This is because the subcarrier 26 is in a fade notch and, since it is in between two of the comb pilot positions, the interpolation is not able to estimate this subcarrier properly.

In order to further quantify the performance of the estimators over time and frequency, we calculate the MSE over the 100 frames per each subcarrier and OFDM symbol as

$$\mathrm{MSE}[m,q] = \frac{1}{F}\sum_{f=1}^{F}\left|h_f[m,q] - \hat{h}_f[m,q]\right|^2. \qquad (6)$$

In (6), the number of transmitted frames is $F = 100$, $m = 1 \ldots 37$ is the OFDM symbol index, $q = 1 \ldots 52$ denotes the subcarrier number, and $h_f[m,q]$ and $\hat{h}_f[m,q]$ are the true channel transfer function for the frame f and its estimate, respectively. We show the results of the MSE calculation in Fig. 8. Comparing Fig. 8 (a) and (c), it can be clearly noticed that the BC-MMSE$_2$ estimator presents less degradation in time than the B-MMSE. On the contrary, the CLS-linear estimator does not show any degradation in time, but some of the subcarriers are not well estimated, and thus have a high MSE.

IV. Conclusions

We presented the results of a PHY-layer 802.11p simulator using a realistic non-stationary vehicular channel model. We have shown that the channel estimation performance is strongly influenced mainly by two factors: the diffuse components strength, and the SNR. Whereas comb-based estimators perform best in environments with rich diffuse components and high SNR, they do not reach a satisfactory result for low SNRs. On the other hand, we find that block- based channel estimators perform well in the opposite case. The phase evolution is well estimated in the comb-type estimators, but a phase offset is present in almost subcarriers. This phase offset stays within ± 45 degrees which is the phase separation between symbols for the used QPSK modulation, and consequently no wrong symbol decisions are made for the used modulation. Due to the frequency separation between comb-pilots, fade notches can not be estimated. We expect to achieve much better results using a midamble, which will allow to track changes in time for all subcarriers.

References

[1] S. Eichler, "Performance evaluation of the IEEE 802.11p WAVE communication standard," in *Vehicular Technology Conference, 2007. VTC-2007 Fall. 2007 IEEE 66th*, pp. 2199–2203, 30 2007-Oct. 3 2007.

[2] M. Amadeo, C. Campolo, A. Molinaro, and G. Ruggeri, "A WAVE-compliant MAC protocol to support vehicle-to-infrastructure non-safety applications," in *Communications Workshops, 2009. ICC Workshops 2009. IEEE International Conference on*, pp. 1–6, June 2009.

[3] G. Kiokes and N. Uzunoglu, "Development of a simulation environment for vehicular communications, implementation of FEC coding chain in xilinx FPGA based on IEEE 802.11p standard," in *IEEE International Symposium on a World of Wireless, Mobile and Multimedia Networks & Workshops, 2009. WoWMoM 2009.*, pp. 1–3, June 2009.

[4] J. Karedal, F. Tufvesson, N. Czink, A. Paier, C. Dumard, T. Zemen, C. Mecklenbräuker, and A. Molisch, "A geometry-based stochastic MIMO model for vehicle-to-vehicle communications," *Wireless Communications, IEEE Transactions on*, vol. 8, pp. 3646–3657, July 2009.

[5] I. S. 802.11p/D9.0, "Specific requirements part 11: Wireless LAN medium access control (MAC) and physical layer (PHY) specifications amendment 7: Wireless access in vehicular environments," July 2009.

[6] J. van de Beek, O. Edfors, M. Sandell, S. Wilson, and P. Borjesson, "On channel estimation in OFDM systems," in *Vehicular Technology Conference, 1995 IEEE 45th*, vol. 2, pp. 815–819 vol.2, Jul 1995.

[7] Y. Shen and E. Martinez, "Channel estimation in OFDM systems," January 2006.

[8] S. Coleri, M. Ergen, A. Puri, and A. Bahai, "Channel estimation techniques based on pilot arrangement in OFDM systems," *Broadcasting, IEEE Transactions on*, vol. 48, pp. 223–229, Sep 2002.

[9] A. Doukas and G. Kalivas, "Performance analysis of a channel estimator using linear interpolation for OFDM systems," in *Signals, Systems and Computers, 2006. ACSSC '06. Fortieth Asilomar Conference on*, pp. 1786–1790, 29 2006-Nov. 1 2006.

[10] J. Park, J. Kim, C. Kang, and D. Hong, "Channel estimation performance analysis for comb-type pilot-aided OFDM systems with residual timing offset," in *Vehicular Technology Conference, 2004. VTC2004-Fall. 2004 IEEE 60th*, vol. 6, pp. 4376–4379 Vol. 6, Sept. 2004.

[11] A. Molisch, *Wireless Communications*. John Wiley & Sons Ltd., 2005.

[12] A. Paier, J. Karedal, N. Czink, H. Hofstetter, C. Dumard, T. Zemen, F. Tufvesson, C. F. Mecklenbräuker, and A. F. Molisch, "First results from car-to-car and car-to-infrastructure radio channel measurements at 5.2 GHz," in *International Symposium on Personal, Indoor and Mobile Radio Communications (PIMRC) 2007*, September 2007.